Research Square

Preprints are preliminary reports that have not undergone peer review.
They should not be considered conclusive, used to inform clinical practice,
or referenced by the media as validated information.

# Carbon tetrachloride (CCl4) accelerated development of non-alcoholic fatty liver disease (NAFLD)/steatohepatitis (NASH) in MS-NASH mice fed western diet supplemented with fructose (WDF)

**Guodong Zhang**
Crown Bioscience, Inc.
**Xiaoli Wang**
Crown Bioscience Inc
**Tzu-Yang Chung**
Crown Bioscience Inc
**Weiwei Ye**
Crown Bioscience Inc
**Lauren Hodge**
Crown Bioscience Inc
**Likun Zhang**
Crown Bioscience Inc
**Keefe Chng**
Crown Bioscience Inc
**Yong-Fu Xiao**
Crown Bioscience Inc
**Yixin Wang** ( yxwang2000@gmail.com )
Crown Bioscience Inc https://orcid.org/0000-0002-3466-429X

**Research article**

**Keywords:** NAFLD, NASH, FATZO, high fat diet, liver fibrosis, hepatosteatosis, inflammation

**Posted Date:** June 1st, 2020

**DOI:** https://doi.org/10.21203/rs.3.rs-30324/v1

**License:** This work is licensed under a Creative Commons Attribution 4.0 International License.
Read Full License

**Version of Record:** A version of this preprint was published on October 15th, 2020. See the published version at https://doi.org/10.1186/s12876-020-01467-w.

## Abstract

# Background

Multiple NAFLD/NASH murine models have been developed by obesogenic diets and/or chemical induction. MS-NASH (formally FATZO) mouse is a spontaneously developed dysmetabolic strain that can progress from hepatosteatosis to moderate fibrosis when fed western diet supplemented with 5% fructose (WDF). This study aimed to use carbon tetrachloride ($CCl_4$) to accelerate and aggravate progression of NAFLD/NASH in MS-NASH mouse.

# Methods

Male MS-NASH mice at 8 weeks of age were fed WDF for the entire study. Starting at 16 weeks of age, $CCl_4$ was intraperitoneally administrated twice weekly at a dose of 0.2 mL/kg for 3 weeks or 0.08 mL/kg for 8 weeks. Obeticholic acid (OCA, 30 mg/kg, QD) was administered in both MS-NASH and C57Bl/6 mice fed WDF and treated with $CCl_4$ (0.08 mL/kg).

# Results

WDF enhanced obesity and hepatosteatosis, as well as induced moderate fibrosis in MS-NASH mice similar to that reported previously. Administration of $CCl_4$ accelerated liver fibrosis with increased bridging, but no significant impact on liver steatosis and lipid contents. Compared to the high dose $CCl_4$ at 0.2 mL/kg, the lower dose of 0.08 mL/kg caused less death and smaller elevation of ALT and AST. Compared to MS-NASH mice, C57Bl/6 mice with WDF and $CCl_4$ (0.08 mL/kg) resulted in milder hepatosteatosis and fibrosis. OCA treatment significantly lowered liver triglycerides, steatosis and fibrosis in both MS-NASH and C57Bl/6 mice treated with WDF and $CCl_4$.

# Conclusions

CCl4 reduced induction time and exacerbated the fibrosis in MS-NASH mice on WDF, which, thus, becomes a superior NASH model with more prominent liver pathology used favorably in pharmaceutical industry for testing novel therapeutics targeting NASH.

## Background

Nonalcoholic fatty liver disease (NAFLD) is the most prevalent complications in metabolic diseases, comprising a cluster of conditions spanning from early hepatic steatosis to late stage cirrhosis in the absence of alcohol consumption [1, 2]. While simple steatosis with minimal inflammation has no clinical implications, nonalcoholic steatohepatitis (NASH) with lobular inflammation has serious consequences

as it progresses to liver fibrosis in 10–20% of cases, leading to cirrhosis and possible hepatocellular carcinoma (HCC) [3]. A two-hit model of pathogenesis has been widely accepted for the development of NASH from liver steatosis that requires 2 sequential events; first, hepatic fat accumulation results in both macrovesicular (adipocytes accumulation) and microvesicular (hepatocyte ballooning) steatosis [4], followed by exposure the accumulated hepatic lipids to hepatic oxidative stress [5, 6] causing lipid peroxidation to release lipid peroxides, which then leads to hepatocyte damage [7–9].

Multiple NAFLD/NASH murine models have been developed by obesogenic or nutrient-deficient diets, chemical induction, genetic modification, or a combination of these manipulations [10–16]. MS-NASH, formerly published as FATZO, mouse [17], was developed by crossing C57Bl/6 and AKR/J strains as a new generation animal model spontaneously developing obesity, metabolic disorders and hyperglycemia under normal diet in the presence of an intact leptin signaling pathway, beginning to exhibit glucose intolerance, insulin resistance and hyperinsulinemia as early as 6 weeks of age, but not spontaneously developing NASH/NAFLD [18, 19]. Western (high fat) diet supplemented with fructose (WDF) has been utilized to induce NASH/NAFLD in murine models [10, 15, 20]. When MS-NASH mice are fed WDF, they develop NAFLD/NASH phenotypes with elevation of plasma ALT/AST and lipid levels as early as 4 weeks, an increase in liver triglycerides at ~ 12 weeks, and exhibition of hepatic steatosis, ballooning, inflammation and mild to moderate fibrosis at ~ 20 weeks [21]. In recent years, MS-NASH mice on WDF have been used as an improved translational model of obesity, metabolic disorders and diabetes as well as NAFLD/NASH in drug discovery and development. However, the NASH induction time is relatively long (~ 20 weeks) with relatively moderate liver fibrosis (pathology score ~ 1).

Carbon tetrachloride ($CCl_4$) is a well-known liver toxin that causes direct hepatocyte injury, leading to liver fibrosis and HCC [22–24]. Administration of $CCl_4$ in C57Bl/6 mice has been shown to cause liver fibrosis [25]. Furthermore, administration of $CCl_4$, in high fat diet-induced obesity (DIO) model in C57Bl/6 mice resulted in histopathological features of NASH, increased serum ALT and liver hydroxyproline [26]. Although moderately effective in modeling aspects of NASH, C57Bl/6 strain lacks the features of dysmetabolism and diabetes, which typically accompany NAFLD/NASH etiology in humans [13, 14].

The aim of the present study is to use $CCl_4$ in MS-MASH mice fed WDF to accelerate the disease progression by reducing the induction time and exacerbating liver fibrosis while maintaining metabolic disorders, hepatosteatosis and other phenotypes of NASH/NAFLD seen in human, such as obesity, metabolic disorders, insulin resistance, diabetes, etc.

# Methods

# Animals

Male MS-NASH (formally FATZO) mice [17] were developed by Crown Bioscience as the new generation of mouse model with obese, metabolic disorder, diabetes and NAFLD/NASH that is more translatable to human diseases [18, 19]. The animals for this study were bred, housed individually in IVC cages (Taicang,

China) or open ventilated cages (Indianapolis, IN), and fed control diet (CD, Purina 5008 chow, LabDiet, St. Louis, MO) with distilled water ad libitum for the first 8 weeks after birth, then, stratified into different experimental groups based on body weight, serum ALT and AST. Room temperature was monitored and maintained at 22–26 °C with a 12-hour light cycle (06:00–18:00). C57Bl/6J mice (The Jackson Laboratory, Ellsworth, Maine) were used as control strain and housed under the same conditions. All mice were maintained and treated in accordance with the guidelines of Association for Assessment and Accreditation of Laboratory Animal Care (AAALAC), and experimental protocols approved by the Institutional Animal Care and Use Committee (IACUC).

## Effects of $CCl_4$ in MS-NASH mice fed Western diet supplemented with fructose (WDF)

## The first study aimed to, 1) confirm the characterization of MS-NASH mice fed WDF (40% kCal fat, 43% kCal carbohydrate, 17% kCal protein, D12079B, Research Diets, New Brunswick, NJ) to induce liver phenotypes; and 2) examine the dose effect of $CCl_4$ (diluted in olive oil, Sigma Aldrich) injected intraperitoneally (IP) twice a week to shorten the induction time and to enhance liver fibrosis.

*High does $CCl_4$ (0.2 mL/kg*, 2% v/v*) for 3 weeks*: After 8 weeks on CD, MS-NASH mice were divided into: 1) CD (n = 8): continued on CD for the rest of 11 weeks; 2) WDF (n = 8); and 3) WDF + $CCl_4$ (n = 6): switched to WDF for the rest of 11 weeks to induce liver phenotypes; after 8 weeks on WDF, vehicle or $CCl_4$ was injected IP twice weekly for 3 weeks, respectively.

*Low dose $CCl_4$ (0.08 mL/kg, 5.33% v/v) for 8 weeks* After 8 weeks on CD, MS-NASH mice were switched to WDF for 16 weeks to induce liver phenotypes, which were divided at 8

weeks after WDF into 2 groups: 1) WDF (n = 4); and 2) WDF + $CCl_4$ (n = 11).

## Effects of OCA in mice fed WDF plus $CCl_4$

After 8 weeks on CD, MS-NASH mice were fed WDF for 16 weeks to induce liver phenotypes. After 8 weeks on WDF, the animals were injected IP with low dose $CCl_4$ (0.08 mL/kg) and divided into vehicle (n = 11) and OCA (n = 10) groups for an additional 8 weeks during which, vehicle (1% methylcellulose, Sigma Aldrich) or OCA (Toronto Research Chemicals, New York, ON, Canada, 30 mg/kg) was administrated orally once daily. C57Bl/6 mice were compared with the same protocol in vehicle (n = 9) or OCA (n = 9) groups.

# Sample collection, processing and measurements

In all the above experiments, body weights were recorded every 4 weeks. At the end of the experiments, all mice were euthanized by $CO_2$ inhalation and confirmed with cervical dislocation approximately 24 hours after the last $CCl_4$ administration.

*Blood* samples Blood samples during the course of the experiment were collected from the tail or at the end of the experiment from cardiac puncture, from which, serum prepared for measuring AST and ALT by a clinical analyzer (Beckman-Coulter AU480; Brea, CA). In the low dose $CCl_4$ repeated treatment group, in-life blood samples were taken ~ 24 hours, and terminal blood samples taken, ~ 24 hours after $CCl_4$ doing, respectively. A separate experiment was performed to observe the acute time course at 24, 48 and 72 hours in response to a single dose of $CCl_4$ at 0.2 mL/kg in SM-NASH mice on CD.

*Liver* contents The right lobe of the liver (~ 200 mg/animal) was collected and snap frozen in liquid nitrogen, placed in Lysing Matrix D Tubes with distilled water at 20% concentration (MP Biomedicals, Santa Anna, CA), homogenized in a Fastprep-FP120 cell disrupter (Thermo Fisher Savant) in cold condition for 30 seconds. The liver contents of triglyceride and cholesterol were analyzed by a clinical analyzer (Beckman-Coulter AU480) within 30 min of sample preparation.

*Liver histology* The left lobe of the liver was fixed in 10% neutral buffered formalin for 24 hours followed by bath in alcohol then xylene for paraffin embedding, cut with 5-µm section and stained with Hematoxylin and Eosin (H&E) and Picro Sirius Red (PSR). A whole slide digital imaging system (Aperio Scan Scope CS system, 360 Park Center Drive, Vista, CA) was used to scan the slides at 20x in 1.5 to 2.25 min.

# Liver Histopathology analysis

*Semi-quantitative scoring by a pathologist* The digital images were evaluated by a well-trained research pathologist blind of different study groups with the standard NASH criteria for semi-quantitative scoring commonly used in preclinical animal models and in patients [27, 28]. Hepatosteatosis, lobular inflammation, and hepatocyte balloon degeneration were scored individually from the H&E staining and then summarized as a standard NAFLD Activity Score (NAS). Fibrosis score was assessed systemically with pattern recognition from PSR staining. Three representative areas per liver were examined and the scores of each parameter from individual animal were averaged.

*Computerized quantitative analysis* Computer software with automatic intelligence (AI) machine learning algorithm for histology analysis from Halo (Indica Labs, Albuquerque, NM) or ImageDx (Reveal Biosciences, San Diego, CA) were used to analyze digitally scanned images of H&E and PSR staining for quantitative analysis of steatosis, ballooning, inflammation or fibrosis in a set of the same slides evaluated by the pathologist. The analysis process included automated tissue identification, followed by segmentation of regions of interest for quantification of the following metrics: 1) Steatosis percentage: the area of total lipid accumulation subcategorized micro- or macro-vesicular within the entire section area; 2) Ballooning hepatocyte density: the density of ballooning hepatocytes within the entire section area; 3) Inflammatory cell density: the total number of inflammatory cells within the entire section area. All 3 parameters above were analyzed in the H&E stained Sect. 4) Fibrosis percentage: the total fibrosis area within the entire section area in the PSR stained section.

# Statistical analysis

All values are reported as Mean ± standard error of mean (SEM), unless noted otherwise. Model characterization were compared in MS-NASH mice on CD or

WDF with or without $CCl_4$; and effects of OCA were compared to vehicle with One-Way ANOVA for multiple groups or Holm-Sidak t-test for 2 groups. Survival curves of total MS-NASH mice and C57Bl/6 mice were compared using Log-rank test for trend. Parametric correlation tests were conducted between pathologist scores and ImageDx quantitative analysis using Pearson correlation coefficient r. Statistical differences were denoted as two-sided $p < 0.05$ or $p < 0.005$. Prism software (GraphPad, version 8.3) was used for the statistical analysis and graphing.

## Results

### Dose effects of $CCl_4$ in MS-NASH mice fed western diet supplemented with fructose (WDF)

#### *High dose $CCl_4$ (0.2 mL/kg), twice weekly for 3 weeks*

Similar to the previous report in MS-NASH mice [21], the present data confirmed that compared to the control diet (CD), WDF enhanced the obesity phenotype (Fig. 1a) with reduction in food (Fig. 1b), but not caloric (Fig. 1c) intake, however, it significantly elevated serum ALT (Fig. 1d) and AST (Fig. 1e).

To establish the proper dose of $CCl_4$ that can accelerate disease progression and enhance liver fibrosis without significant toxic impact on MS-NASH mice, a dose of $CCl_4$ at 0.2 mL/kg twice weekly was selected, which was a relatively low dose compared to those reported in many studies to induce liver fibrosis in normal rodents without steatosis [13, 22]. Compared to MS-NASH mice on CD or WDF without $CCl_4$, administration of $CCl_4$ significantly reduced body weight (Fig. 1a), food (Fig. 1b) and caloric (Fig. 1c) intake, as well as dramatically elevated ALT

(Fig. 1d) and AST (Fig. 1e) measured ~ 24 hours after the last dose of $CCl_4$. The acute response of ASL and ALT to a single dose of $CCl_4$ at 0.2 mL/kg in a separate experiment showed a similar elevation at 24 hours, but quickly diminished on day 2 and 3 (Fig. 1f).

The representative histopathology images showed relatively normal liver in MS-NASH mice on CD (Fig. 2a & b), but a typical NAFLD/NASH pathology in MS-NASH mice on WDF with significantly increased macrovesicular fatty accumulation and microvesicular hepatocyte ballooning (Fig. 2c & d), which is similar to what we reported earlier [21]. Although Fig. 2e & f showed that $CCl_4$ administration in MS-NASH mice on WDF aggravated liver injury and centrilobular fibrosis, pathology scores evaluated by the pathologist failed to detect such enhanced pathology in steatosis, inflammation, ballooning and overall NAS scores from H&E images (Fig. 2g), nor the fibrosis score from PSR images (Fig. 2h, left). However, a quantitative measurement of fibrotic area by computer analysis software (Halo) from PSR images showed a significantly greater fibrosis area in the $CCl_4$ (~ 8%) than CD or WDF (~ 2%) group (Fig. 2h, right).

*Low dose $CCl_4$ (0.08 mL/kg), twice weekly for 8 weeks*

To further reduce the toxicity of $CCl_4$, a separate experiment was performed with the dose of $CCl_4$ reduced to 0.08 mL/kg twice weekly in MS-NASH mice on WDF. Compared to the mice without $CCl_4$, low dose $CCl_4$ reduced

body weight (Fig. 3a), while the elevation of serum ALT (Fig. 3b) and AST (Fig. 3c) was not as dramatic compared to those with high dose $CCl_4$ measured ~ 24 hours after the last dose of $CCl_4$ at the end of the experiment. When in-life monitoring of serum ALT and AST was performed 3 days after $CCl_4$ dosing to minimize influence from acute raise of enzyme levels shown in the high dose experiment, serum ALT and AST levels on week 12 and 14 in the $CCl_4$ group was significantly lower compared with the mice on WDF only, yet it was still higher than their own baseline before WDF feeding. The liver weight (Fig. 3d) and contents of cholesterol (Fig. 3e), but not triglycerides (Fig. 3f) were significantly reduced by $CCl_4$.

MS-NASH mice on WDF without $CCl_4$ showed similar histopathology characteristics as reported earlier [21] with significant steatosis (Fig. 4a) and moderate fibrosis (Fig. 4b). However, MS-NASH mice on WDF treated with $CCl_4$ presented persisting hepatosteatosis and hepatocyte ballooning degeneration in H&E stained images (Fig. 4c), as well as typical perisinusoidal and periportal fibrosis, along with enhanced bridging fibrosis in PSR stained images (Fig. 4d). The NAS and fibrosis scores evaluated by the pathologist (Fig. 4e) showed significantly aggravated liver fibrosis with little influence on other aspects of liver pathology by low dose $CCl_4$. Similar to the pathology score analysis, an independent computerized quantitative analysis by Reveal ImageDx also showed larger fibrosis area in mice with $CCl_4$ compared to those without, but no

significant difference in the steatosis area and inflammatory cell infiltration and degenerated liver cell counts between the 2 groups (Fig. 4f).

## Therapeutic effects of Obeticholic acid (OCA) in MS-NASH or C57Bl/6 mice on WDF treated low dose $CCL_4$ (0.08 mL/kg) twice weekly for 8-weeks

Obeticholic Acid (OCA, 30 mg/kg, QD) or vehicle was administered orally in MS-NASH or C57Bl/6 mice fed WDF and treated with $CCl_4$ (0.08 mL/kg) twice weekly for 8 weeks. Compared to the vehicle groups, OCA had no significant effect on body weight (Fig. 5a) and serum ALT level (Fig. 5b) in both MS-NASH and C57Bl/6 mice, but lowered AST only in C57Bl/6 in mice (Fig. 5c). However, OCA significantly reduced liver contents of triglycerides (Fig. 5e) and cholesterol (Fig. 5f) in both MS-NASH and C57Bl/6 mice, and reduced liver weight only in MS-NASH mice (Fig. 5d).

Histopathology images of OCA treated mice (Fig. 6c, d, g & h) showed less lipid vacuoles and alleviated bridging fibrosis compared to the vehicle treated mice (Fig. 6a, b, e & f). These observations were confirmed by both pathologist scoring (Fig. 6j) and computerized quantification (Fig. 6k). Steatosis score by pathologist and percent area by computer quantification were significantly reduced by OCA treatment in both MS-NASH and C57Bl/6 mice; quantitative infiltrated inflammatory cell counts in C57Bl/6 mice and degenerated ballooning hepatocyte counts in MS-NASH mice were significantly reduced by OCA

treatment; NAS and fibrosis scores were significantly reduced in MS-NASH mice by OCA treatment; and percentage fibrosis area was significantly reduced by OCA treatment in both MS-NASH and C57Bl/6 mice. Both pathology score and quantitative analysis showed lower NAS and fibrosis scores in C57Bl/6 compared to MS-NASH mice, indicating that C57Bl/6 mice may require longer NASH induction time and have less hepatocyte ballooning degeneration.

## Survival rate in MS-NASH and C57Bl/6 mice on WDF and treated high and low dose of $CCL_4$

The majority of the mortality occurred in the first 3 weeks of $CCl_4$ administration in both MS-NASH and C57Bl/6 mice. High dose $CCl_4$ caused death in ~ 20% MS-NASH mice within the first 3 weeks, leading to early termination of the first experiment (Fig. 7). The survival rate in MS-NASH mice under lower dose $CCl_4$ surpassed those under high dose $CCl_4$ in the first 3 weeks and reached 87.5% at the end of entire 8-week experimental duration. The survival rate tended to be lower in 57Bl/6 than MS-NASH mice with low dose $CCl_4$. However, this trend was not statistically significant among all the groups.

# Correlation of imagining analysis between the pathology score and computerized quantification

A simple linear correlation analysis was performed on 4 aspects of histology readouts between pathologist scoring and quantitative image analysis with ImageDx software. Steatosis (Fig. 8a), lobular inflammation (Fig. 8b), hepatocyte ballooning degeneration (Fig. 8c) and fibrosis (Fig. 8d) scores all showed significant correlations between the 2 independent analyses.

## Discussion

The present data confirmed our previous report that MS-NASH mice possess all features of metabolic disorders [18, 19] and NAFLD/NASH when on WDF [21], however, with a relatively long induction duration (~ 20 weeks), and moderate liver fibrosis (pathology score ~ 1). Low dose $CCl_4$ (0.08 mL/kg) accelerated the progression of NASH in ~ 8 weeks and exacerbated liver fibrosis by raising the pathology score to ~ 4, but not significantly affecting other features of liver pathology measured by NAS in MS-NASH mice on WDF. Consistent with preclinical and clinical reports [16, 29–31], OCA treatment reduced NASH pathology in this model and surpassed the therapeutic effects on previous WDF only model [21]. Thus, MS-NASH mice on WDF and $CCl_4$ is an appropriate translational model for testing novel therapeutics targeting NASH/NAFLD.

The pathogenesis of NAFLD/NASH is initiated by systemic dysmetabolism, leading to lipid accumulation, hepatosteatosis, hepatocyte ballooning [4], inflammatory cell infiltration, increase in oxidative stress [5, 6], hepatocytes injury, fibrosis, etc. [7–9]. $CCl_4$ is a known liver toxin directly causing hepatocyte injury, leading to liver fibrosis, cirrhosis and carcinoma, which often requires relatively high doses from 0.2 to 5 mL/kg [22]. In order to avoid aggressive direct hepatocyte injury overshadowing development of hepatosteatosis, a critical component of NAFLD/NASH in MS-NASH mice, $CCl_4$ at 0.2 mL/kg was selected in the first experiment, which, however, caused excessive animal death in the first 3 weeks, probably due to acute liver toxicity evidenced by significant weight loss, reduction of food and caloric intake as well as massive elevation of ALT and AST, but did not significantly affect liver pathology measured by steatosis, ballooning and overall NAS or fibrosis score. When the dose of $CCl_4$ was further reduced to 0.08 mL/kg, although the animals still lost weight, most survived with ALT and AST levels not as high as that in high dose $CCl_4$ group.

Although several noninvasive imaging methods have been used to assist diagnoses of NAFLD/NASH in clinical and preclinical research [32–35], histopathological examination is still the gold standard, especially to differentiate NASH from simple steatosis [28, 36, 37]. In preclinical research with rodent models, postmortem histopathological examination of liver tissue is still a commonly used method, in which the NAFLD Activity Score (NAS) is semi quantitatively evaluated by pathologists for assessment of NAFLD to distinguish steatosis from NASH [28]. NAS provides a composite score based on the degree of steatosis, lobular inflammation, and hepatocyte ballooning with a score $< 2$ unlikely and $\geq 5$ likely representing NASH, respectively. The present liver histopathology in MS-NASH mice on WDF exhibited persisting macrovesicular steatosis, hepatocyte ballooning degeneration, and inflammatory cell infiltration with the NAS scores ~ 5, thus, it qualifies as a NSAH model (Figs. 2 & 4). The NAS does not include fibrosis score, with the latter being reported separately on a scale from 0 (without fibrosis) to 4 (cirrhosis) [28], which does not always correlate with each other [27]. In the present experiment, the fibrosis scores were relatively low, only ~ 1.2 in MS-NASH mice for a total duration of 16 weeks on WDF, which, however, was raised to ~ 3 by combination of low dose $CCl_4$ for 8 weeks (Figs. 4 & 6), but not by high dose $CCl_4$ for 3 weeks (Fig. 2h). We suspect a longer duration may be needed for fibrosis development to the level detectable by the pathology scoring system due to its low sensitivity and resolution. The Pathology fibrosis score criteria from 1 to 3 also depends on zonal distribution of fibrotic

findings, with a score of 1 being periportal fibrosis; a score of 2 being periportal and perisinusoidal fibrosis; and a score of 3 being bridging fibrosis between multiple fibrotic areas. MS-NASH mice on WDF develop perilobular fibrosis initially, while $CCl_4$-induced liver fibrosis exhibits centrilobular distribution characteristics. As showed in the present results, a correct combination of these 2 insults (WDF + $CCl_4$) can yield aggravated fibrosis at multiple zones and accelerated bridging between areas.

Furthermore, the semiquantitative pathology scoring system with manually slide reading by pathologists is not only time-consuming and labor-intensive, but also subjective with person to person deviation, and lacks resolution and sensitivity to detect subtle difference in different animal models, different disease stages, and subtle changes by therapeutic intervention. With development of computerized imaging analysis and machine learning technology, commercial software is now available for automatic quantification of histopathology images, including liver pathology for NASH research [31, 38, 39]. As shown in Fig. 2h, the semi-quantitative fibrosis score ~ 1 may be too low to distinguish any differences among treatment groups. However, quantitative image analysis is able to measure the relative area of fibrosis over the entire section as ~ 2% in the control group, and increased to ~ 8% by high (Fig. 2h) or low (Fig. 4f & 6 k) dose $CCl_4$ in MS-NASH mice on WDF. Furthermore, the present data also showed high correlation between a computer quantification and the pathology scores for steatosis, ballooning, inflammation and fibrosis (Fig. 8). Thus, the computerized image analysis is a valid method that is more efficient and consistent, providing higher sensitive and less subjective quantification of histopathology changes in NASH research.

Farnesoid X receptors like OCA has been used in preclinical treatment for diet [16] or chemical [40] induced liver fibrosis and NASH. The present data demonstrated a more robust efficacy of OCA treatment in MS-NASH mice on both WDF and $CCl_4$ compared to those on WDF alone [21], which might be due to the model with a more robust liver fibrosis or OCA with dual alleviation to both diet/chemical-induction.

Mitochondrial metabolism dysregulation has been implicated in NALFD pathogenesis and progression with reduced capacity to compensate for increased oxidative stress, a key factor in hepatic injury and fibrosis, although the precise disease etiology remains to be further investigated [41]. Accumulating evidence suggests that therapeutically targeting the mechanisms leading to mitochondrial dysfunction may have therapeutic benefits to patients with liver disease [42–45]. The present survival analysis data showed that MS-NASH mice better tolerated $CCl_4$ associated mortality compared to C57Bl/6 mice, which could be attributed to higher catalase activity to oxidative stress, thus, reducing oxidative DNA damage in MS-NASH mice reported by Boland et. al [46].

The present data also demonstrated that the degree of NASH pathology measured by both NAS and fibrosis scores from the pathologist and computer quantification appeared to be higher in MS-NASH than C57Bl/6 mice on WDF and $CCl_4$, indicating that C57Bl/6 mice may require longer NASH induction time and have less hepatocyte ballooning degeneration, consistent with the view that MS-NASH mouse is a superior NASH model with more prominent hepatosteatosis pathology and metabolic disorders.

## Conclusions

$CCl_4$ at 0.08 mL/kg reduced NASH induction time and exacerbated liver fibrosis formation while maintaining the other pathologic changes such as hepatic steatosis, ballooning, inflammation, etc. in MS-NASH mice on WDF. The NAFLD/NASH phenotypes in this model can also be ameliorated by the treatment of OCA. This yields a translational animal model of NASH that closely mimics human disease, therefore has been used in the pharmaceutical industry for testing novel therapeutic drugs in treatment of NASH and metabolic disorders.

## Declarations

# Ethics approval and consent to participate

All animal experiments in the study were approved by the Institutional Animal Care and Use Committee at Crown Bioscience.

# Consent for Publication

All the authors have carefully read and approved for the submission of the manuscript t0 BMC Gastroenterology for publication. The data reported in the manuscript have not been submitted and are not in the consideration to submit elsewhere for publication except as an abstract form to present in 2020 ADA meeting.

# Availability of data and material

The datasets generated and analyzed during the current study are not publicly available due to potential commercial misuse but are available from the corresponding author on reasonable request.

# Competing interests

The authors declare no competing interests.

# Funding

Not applicable

# Author’s contributions

GZ, XW, YW designed the experiments, analyzed the data and wrote the paper; GZ, XW, TC, WY performed the experiment and analyzed the data; LZ performed the histological evaluation; GZ, XW, LH, KC, YX, YW participated in the discussion and paper writing. All authors have read and approved the manuscript.

# Acknowledgments

The authors gratefully acknowledge Laura Healy of LNH Tox Path Consulting, LLC for their technical assistance in the pathology scoring of the experiments; Laure Rope for reviewing and editing the manuscript.

## Abbreviations

ALT/AST: Aspartate/Alanine aminotransferase; CD:Control diet; CCl4:Carbon; tetrachloride; DIO:Diet-induced obesity; H&E:Hematoxylin and Eosin; HCC:Hepatocellular carcinoma; MS-NASH mouse:Metabolic syndrome-NASH; NAFLD/NASH:Nonalcoholic fatty liver disease/steatohepatitis; NAS:NAFLD activity score; OCA:Obeticholic acid; PSR:Picro Sirius Red; WDF:Western diet supplemented with fructose

## References

1. Ratziu V, Goodman Z, Sanyal A. Current efforts and trends in the treatment of NASH. J Hepatol. 2015;62(1 Suppl):65–75.
2. Younossi ZM, Koenig AB, Abdelatif D, Fazel Y, Henry L, Wymer M. Global epidemiology of nonalcoholic fatty liver disease-Meta-analytic assessment of prevalence, incidence, and outcomes. Hepatology. 2016;64(1):73–84.
3. Younossi ZM, Blissett D, Blissett R, Henry L, Stepanova M, Younossi Y, Racila A, Hunt S, Beckerman R. The economic and clinical burden of nonalcoholic fatty liver disease in the United States and Europe. Hepatology. 2016;64(5):1577–86.
4. Day CP, James OF. Steatohepatitis: a tale of two "hits". Gastroenterology. 1998;114(4):842–5.
5. Maurizio P, Novo E. Nrf1 gene expression in the liver: a single gene linking oxidative stress to NAFLD, NASH and hepatic tumours. J Hepatol. 2005;43(6):1096–7.
6. Sakaida I, Okita K. The role of oxidative stress in NASH and fatty liver model. Hepatol Res. 2005;33(2):128–31.
7. Leclercq IA, Farrell GC, Field J, Bell DR, Gonzalez FJ, Robertson GR. CYP2E1 and CYP4A as microsomal catalysts of lipid peroxides in murine nonalcoholic steatohepatitis. J Clin Invest. 2000;105(8):1067–75.
8. Sumida Y, Niki E, Naito Y, Yoshikawa T. Involvement of free radicals and oxidative stress in NAFLD/NASH. Free Radic Res. 2013;47(11):869–80.
9. Toriniwa Y, Muramatsu M, Ishii Y, Riya E, Miyajima K, Ohshida S, Kitatani K, Takekoshi S, Matsui T, Kume S, et al. Pathophysiological characteristics of non-alcoholic steatohepatitis-like changes in

cholesterol-loaded type 2 diabetic rats. Physiol Res. 2018;67(4):601–12.

10. Abe N, Kato S, Tsuchida T, Sugimoto K, Saito R, Verschuren L, Kleemann R, Oka K. **Longitudinal characterization of diet-induced genetic murine models of non-alcoholic steatohepatitis with metabolic, histological, and transcriptomic hallmarks of human patients**. *Biol Open* 2019, 8(5).
11. Abe N, Tsuchida T, Yasuda SI, Oka K. **Dietary iron restriction leads to a reduction in hepatic fibrosis in a rat model of non-alcoholic steatohepatitis**. *Biol Open* 2019, 8(5).
12. Tsuchida T, Friedman SL. Mechanisms of hepatic stellate cell activation. Nat Rev Gastroenterol Hepatol. 2017;14(7):397–411.
13. Tsuchida T, Lee YA, Fujiwara N, Ybanez M, Allen B, Martins S, Fiel MI, Goossens N, Chou HI, Hoshida Y, et al. A simple diet- and chemical-induced murine NASH model with rapid progression of steatohepatitis, fibrosis and liver cancer. J Hepatol. 2018;69(2):385–95.
14. Tsuchida T, Lee YA, Fujiwara N, Ybanez M, Allen B, Martins S, Isabel Fiel M, Goossens N, Chou HI, Hoshida Y, et al. Corrigendum to "A simple diet- and chemical-induced murine NASH model with rapid progression of steatohepatitis, fibrosis and liver cancer" [J Hepatol 69 (2018) 385–395]. J Hepatol. 2018;69(4):988.
15. Asgharpour A, Cazanave SC, Pacana T, Seneshaw M, Vincent R, Banini BA, Kumar DP, Daita K, Min HK, Mirshahi F, et al. A diet-induced animal model of non-alcoholic fatty liver disease and hepatocellular cancer. J Hepatol. 2016;65(3):579–88.
16. Tolbol KS, Kristiansen MN, Hansen HH, Veidal SS, Rigbolt KT, Gillum MP, Jelsing J, Vrang N, Feigh M. Metabolic and hepatic effects of liraglutide, obeticholic acid and elafibranor in diet-induced obese mouse models of biopsy-confirmed nonalcoholic steatohepatitis. World J Gastroenterol. 2018;24(2):179–94.
17. Neff EP. Farewell, FATZO: a NASH mouse update. Lab Anim (NY). 2019;48(6):151.
18. Droz BA, Sneed BL, Jackson CV, Zimmerman KM, Michael MD, Emmerson PJ, Coskun T, Peterson RG. Correlation of disease severity with body weight and high fat diet in the FATZO/Pco mouse. PLoS One. 2017;12(6):e0179808.
19. Peterson RG, Jackson CV, Zimmerman KM, Alsina-Fernandez J, Michael MD, Emmerson PJ, Coskun T. Glucose dysregulation and response to common anti-diabetic agents in the FATZO/Pco mouse. PLoS One. 2017;12(6):e0179856.
20. Pompili S, Vetuschi A, Gaudio E, Tessitore A, Capelli R, Alesse E, Latella G, Sferra R, Onori P: **Long-term abuse of a high-carbohydrate diet is as harmful as a high-fat diet for development and progression of liver injury in a mouse model of NAFLD/NASH**. *Nutrition* 2020, **75–76**:110782.
21. Sun G, Jackson CV, Zimmerman K, Zhang LK, Finnearty CM, Sandusky GE, Zhang G, Peterson RG, Wang YJ. The FATZO mouse, a next generation model of type 2 diabetes, develops NAFLD and NASH when fed a Western diet supplemented with fructose. BMC Gastroenterol. 2019;19(1):41.
22. Marques TG, Chaib E, da Fonseca JH, Lourenco AC, Silva FD, Ribeiro MA Jr, Galvao FH, D'Albuquerque LA. Review of experimental models for inducing hepatic cirrhosis by bile duct ligation and carbon tetrachloride injection. Acta Cir Bras. 2012;27(8):589–94.

23. Liedtke C, Luedde T, Sauerbruch T, Scholten D, Streetz K, Tacke F, Tolba R, Trautwein C, Trebicka J, Weiskirchen R. Experimental liver fibrosis research: update on animal models, legal issues and translational aspects. Fibrogenesis Tissue Repair. 2013;6(1):19.
24. Scholten D, Trebicka J, Liedtke C, Weiskirchen R. The carbon tetrachloride model in mice. Lab Anim. 2015;49(1 Suppl):4–11.
25. Walkin L, Herrick SE, Summers A, Brenchley PE, Hoff CM, Korstanje R, Margetts PJ. The role of mouse strain differences in the susceptibility to fibrosis: a systematic review. Fibrogenesis Tissue Repair. 2013;6(1):18.
26. Kubota N, Kado S, Kano M, Masuoka N, Nagata Y, Kobayashi T, Miyazaki K, Ishikawa F. A high-fat diet and multiple administration of carbon tetrachloride induces liver injury and pathological features associated with non-alcoholic steatohepatitis in mice. Clin Exp Pharmacol Physiol. 2013;40(7):422–30.
27. Brunt EM, Kleiner DE, Wilson LA, Belt P, Neuschwander-Tetri BA, Network NCR. Nonalcoholic fatty liver disease (NAFLD) activity score and the histopathologic diagnosis in NAFLD: distinct clinicopathologic meanings. Hepatology. 2011;53(3):810–20.
28. Obika M, Noguchi H. Diagnosis and evaluation of nonalcoholic fatty liver disease. Exp Diabetes Res. 2012;2012:145754.
29. Gawrieh S, Guo X, Tan J, Lauzon M, Taylor KD, Loomba R, Cummings OW, Pillai S, Bhatnagar P, Kowdley KV, et al. A Pilot Genome-Wide Analysis Study Identifies Loci Associated With Response to Obeticholic Acid in Patients With NASH. Hepatol Commun. 2019;3(12):1571–84.
30. Thiagarajan P, Aithal GP. Drug Development for Nonalcoholic Fatty Liver Disease: Landscape and Challenges. J Clin Exp Hepatol. 2019;9(4):515–21.
31. Tolbol KS, Stierstorfer B, Rippmann JF, Veidal SS, Rigbolt KTG, Schonberger T, Gillum MP, Hansen HH, Vrang N, Jelsing J, et al. Disease Progression and Pharmacological Intervention in a Nutrient-Deficient Rat Model of Nonalcoholic Steatohepatitis. Dig Dis Sci. 2019;64(5):1238–56.
32. Duman DG, Celikel C, Tuney D, Imeryuz N, Avsar E, Tozun N. Computed tomography in nonalcoholic fatty liver disease: a useful tool for hepatosteatosis assessment? Dig Dis Sci. 2006;51(2):346–51.
33. Irwan R, Edens MA, Sijens PE. Assessment of the variations in fat content in normal liver using a fast MR imaging method in comparison with results obtained by spectroscopic imaging. Eur Radiol. 2008;18(4):806–13.
34. Joseph AE, Saverymuttu SH, al-Sam S, Cook MG, Maxwell JD. Comparison of liver histology with ultrasonography in assessing diffuse parenchymal liver disease. Clin Radiol. 1991;43(1):26–31.
35. Saverymuttu SH, Wright J, Maxwell JD, Joseph AE. Ultrasound detection of oesophageal varices–comparison with endoscopy. Clin Radiol. 1988;39(5):513–5.
36. Lee SS, Park SH. Radiologic evaluation of nonalcoholic fatty liver disease. World J Gastroenterol. 2014;20(23):7392–402.
37. Yin Z, Murphy MC, Li J, Glaser KJ, Mauer AS, Mounajjed T, Therneau TM, Liu H, Malhi H, Manduca A, et al. Prediction of nonalcoholic fatty liver disease (NAFLD) activity score (NAS) with multiparametric

hepatic magnetic resonance imaging and elastography. Eur Radiol. 2019;29(11):5823–31.

38. Han L, Bittner S, Dong D, Cortez Y, Dulay H, Arshad S, Shen W, Kraemer FB, Azhar S. **Creosote bush-derived NDGA attenuates molecular and pathological changes in a novel mouse model of non-alcoholic steatohepatitis (NASH)**. *Molecular and Cellular Endocrinology* 2019, 498.
39. Albadrani M, Seth RK, Sarkar S, Kimono D, Mondal A, Bose D, Porter DE, Scott GI, Brooks B, Raychoudhury S, Nagarkatti M, Nagarkatti P, Jule Y, Diehl AM, Chatterjee S: **Exogenous PP2A inhibitor exacerbates the progression of nonalcoholic fatty liver disease via NOX2-dependent activation of miR21**. *American Journal of Physiology: Gastrointestinal and Liver Physiology* 2019, **317**(4):20.
40. Wang H, Ge C, Zhou J, Guo Y, Cui S, Huang N, Yan T, Cao L, Che Y, Zheng Q, Zheng X, Gonzalez FJ, Wang G, Hao H. Noncanonical farnesoid X receptor signaling inhibits apoptosis and impedes liver fibrosis. EBioMedicine. 2018;37:11.
41. Auger C, Alhasawi A, Contavadoo M, Appanna VD. Dysfunctional mitochondrial bioenergetics and the pathogenesis of hepatic disorders. Front Cell Dev Biol. 2015;3:40.
42. Gusdon AM, Song KX, Qu S. Nonalcoholic Fatty liver disease: pathogenesis and therapeutics from a mitochondria-centric perspective. Oxid Med Cell Longev. 2014;2014:637027.
43. Kalavalapalli S, Bril F, Guingab J, Vergara A, Garrett TJ, Sunny NE, Cusi K. Impact of exenatide on mitochondrial lipid metabolism in mice with nonalcoholic steatohepatitis. J Endocrinol. 2019;241(3):293–305.
44. Sunny NE, Bril F, Cusi K. Mitochondrial Adaptation in Nonalcoholic Fatty Liver Disease: Novel Mechanisms and Treatment Strategies. Trends Endocrinol Metab. 2017;28(4):250–60.
45. Sunny NE, Kalavalapalli S, Bril F, Garrett TJ, Nautiyal M, Mathew JT, Williams CM, Cusi K. Cross-talk between branched-chain amino acids and hepatic mitochondria is compromised in nonalcoholic fatty liver disease. Am J Physiol Endocrinol Metab. 2015;309(4):E311–9.
46. Boland ML, Oldham S, Boland BB, Will S, Lapointe JM, Guionaud S, Rhodes CJ, Trevaskis JL. Nonalcoholic steatohepatitis severity is defined by a failure in compensatory antioxidant capacity in the setting of mitochondrial dysfunction. World J Gastroenterol. 2018;24(16):1748–65.

# Figures

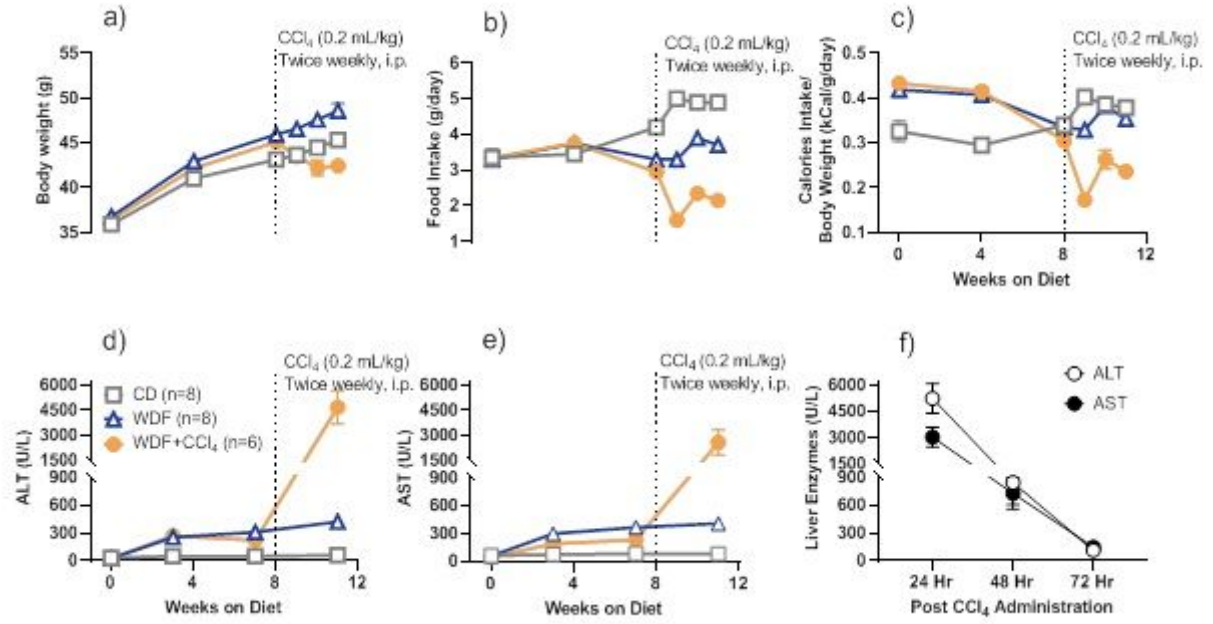


## Figure 1

Effects of high dose CCL4 (0.2 mL/kg) twice weekly for 3 weeks in MS-NASH mice fed Control diet (CD) or Western diet supplemented with fructose (WDF) (a) Body weight; (b) daily food and (c) calories intake; serum (d) ALT and (e) AST before and after repeated high dose CCl4. (f) Time course of acute response of ALT and AST to a single high dose CCL4 in mice on control diet (CD). Data represent as mean ± SEM.

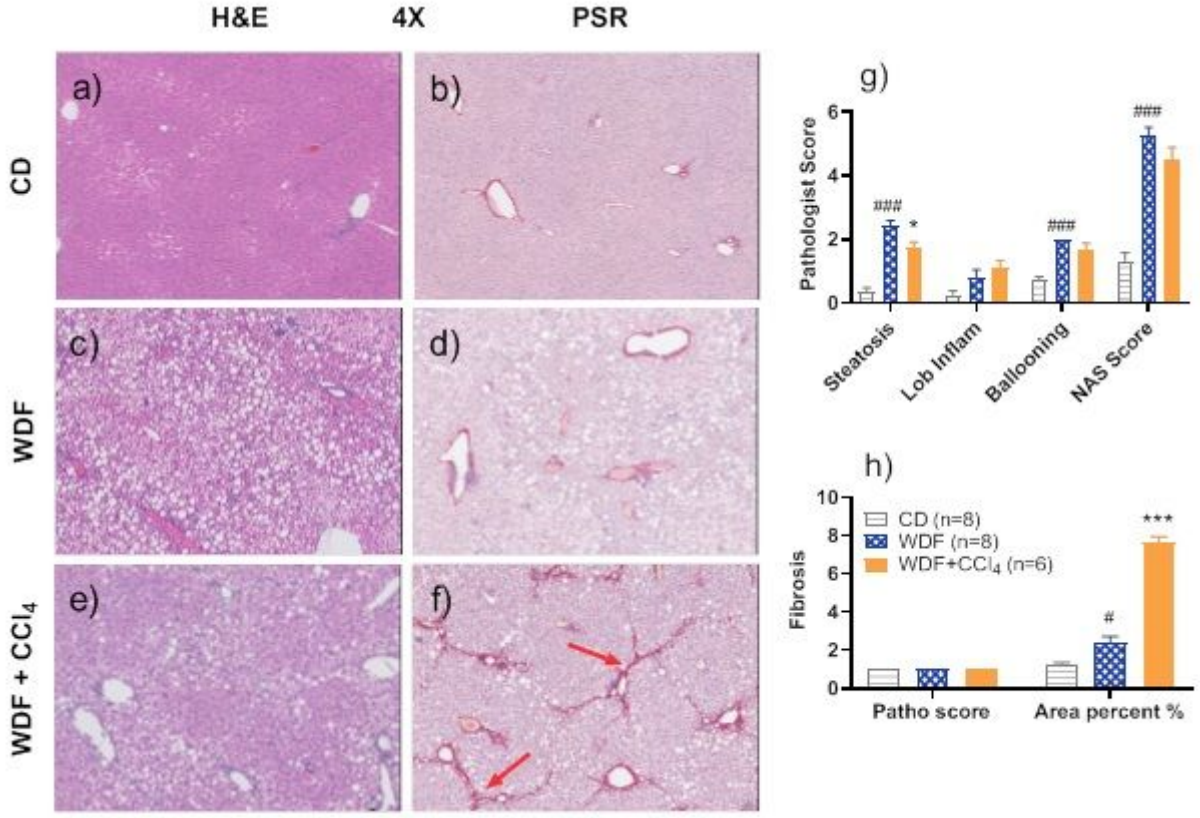

## Figure 2

Histopathology in MS-NASH mice fed Control diet (CD) or Western diet supplemented with Fructose (WDF) treated high dose CCL4 (0.2 mL/kg) twice weekly for 3 weeks Left panel: Representative images of H&E and PSR staining in animals fed (a & b) CD; and WDF treated (c, d) without or (e, f) with CCL4, respectively. Red arrows indicate fibrosis. Right panel: (g) Pathology scores of steatoses (0-3), lobular inflammation (0-3), ballooning (0-2), NAFLD Activity (0-8). (h) left: fibrosis score (0-4) and right: Percentage fibrosis area, quantitatively analyzed as total PSR positive staining area over total liver section area scanned and processed by HALO software. Data represent as mean ± SEM. # p<0.05, ### p<0.005 comparing with CD group; * p<0.05, *** p<0.005 comparing with WDF group by one-way ANOVA analysis.

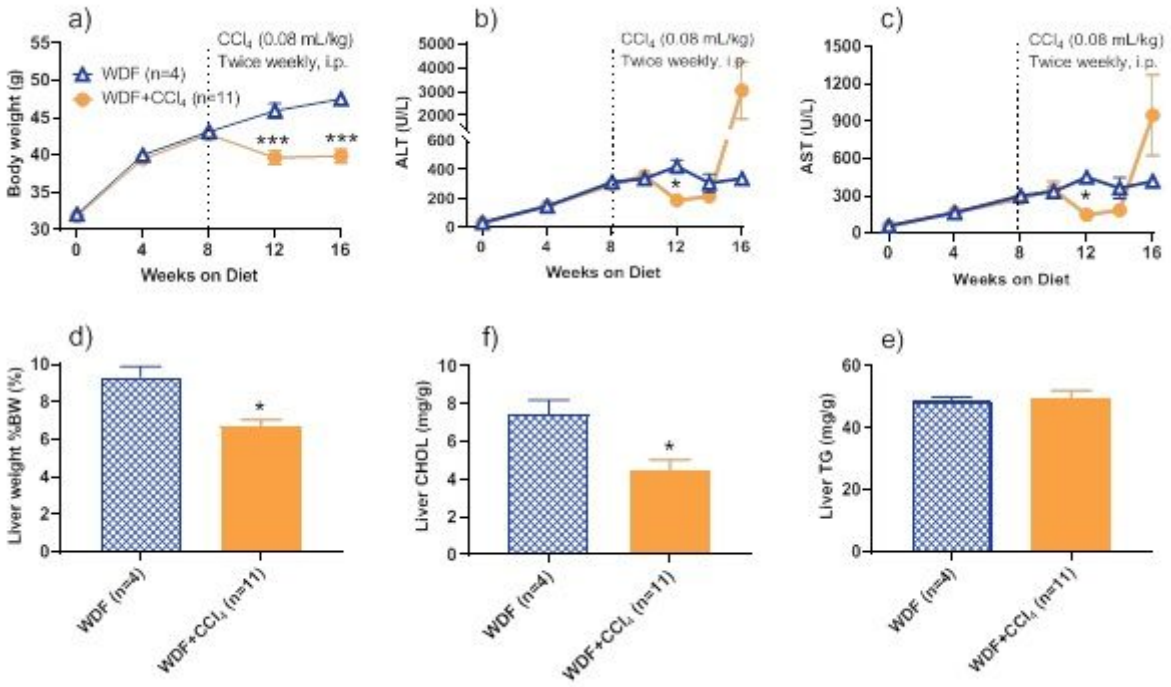


## Figure 3

Effects of low dose CCL4 (0.08 mL/kg) twice weekly for 8 weeks in MS-NASH mice fed Western diet supplemented with fructose (WDF) Top panel: (a) Body weights; serum (b) ALT and (c) AST levels before and after low dose CCL4. In-life AST and AST levels at weeks 11, 12 and 14 were measured ~72 hours; and the terminal one at week 16 measured ~24 hours, after CCl4 administration. Bottom Panel: Liver (d) weight; (e) cholesterol; and (f) triglycerides measured at the end of the study. Data represent as mean ± SEM. * p<0.05, *** p<0.005, WDF vs. WDF + CCl4 group by Holm-Sidak t-test.

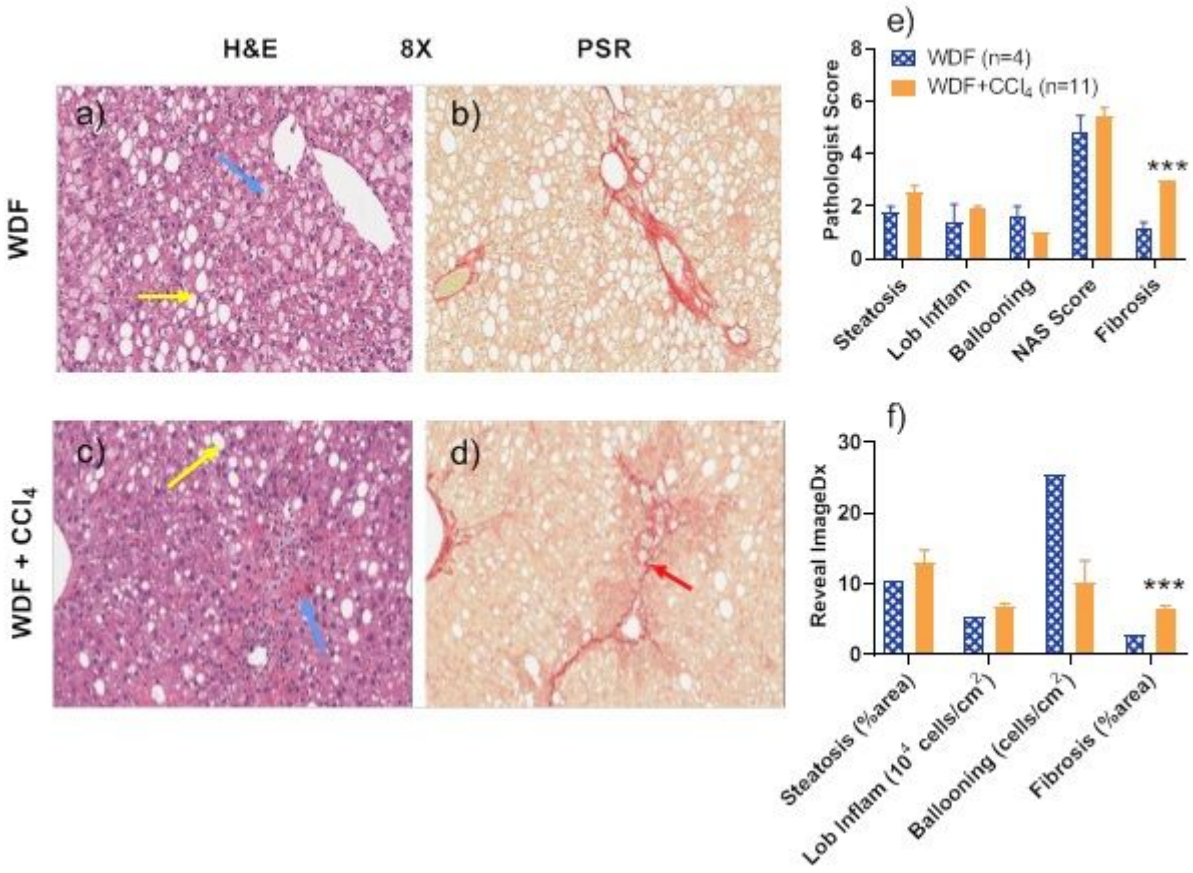


## Figure 4

Histopathology in Western diet supplemented with fructose (WDF) fed MS-NASH mice treated with low dose CCL4 (0.08 mL/kg) for 8 weeks Left panel: Representative images of H&E and PSR staining in animals (a, b) without or (c, d) with CCl4. Yellow arrows indicate macrovesicular vacuolation steatosis; blue arrows indicate microvesicular ballooning; and red arrows indicate fibrosis. Top right panel (e): Pathology scores of steatoses (0-3), lobular inflammation (0-3), ballooning (0-2), and NAFLD activity (0-8), and fibrosis (0-4). Bottom right panel (f): Quantitative histology analyzed as percentage of steatosis and fibrosis area, and cell counts of inflammation and hepatic ballooning by Reveal ImageDx software. Data represented as mean ± SEM. *** $p<0.005$, WDF vs. WDF + CCL4 group using Holm-Sidak t-test.

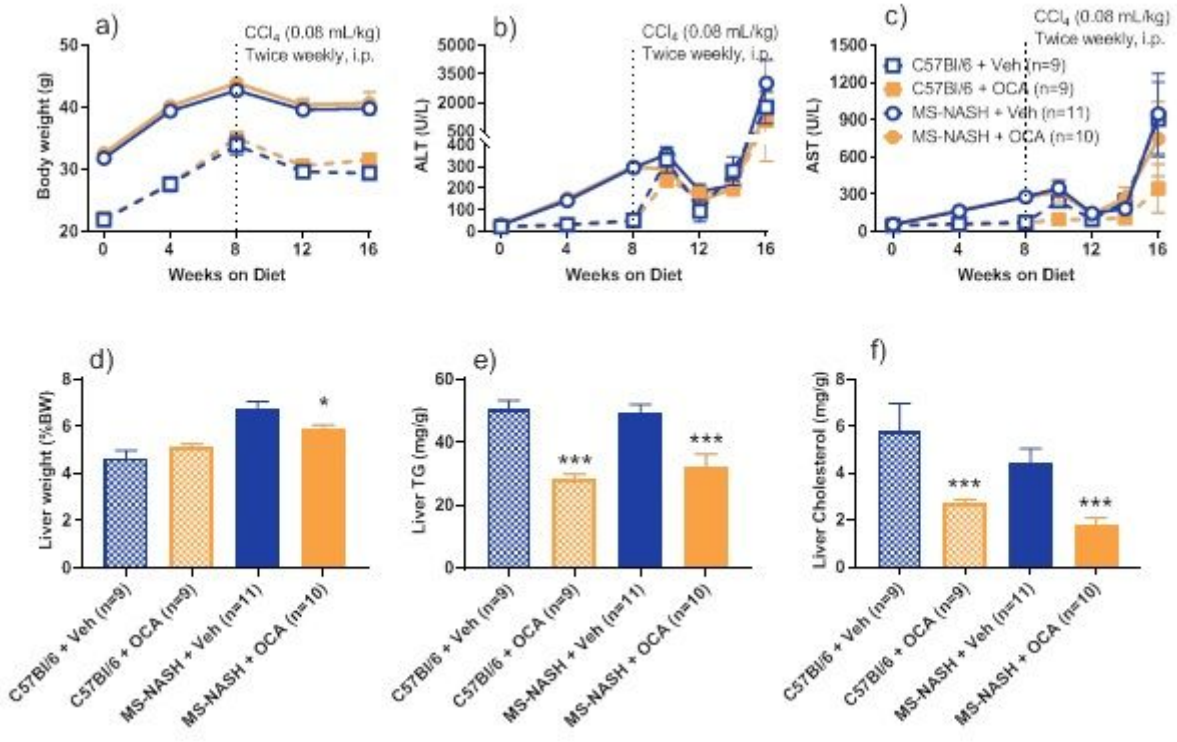


## Figure 5

Therapeutic effects of Obeticholic acid (OCA, 30 mg/kg, QD) in Western diet supplemented with fructose (WDF) fed MS-NASH or C57Bl/6 mice treated low dose CCL4 (0.08 mL/kg) twice weekly for 8 weeks Top panel: (a) Body weight; serum (b) ALT and (c) AST. Bottom panel: (d) Terminal liver weight; (e) triglycerides and (f) cholesterol. Data represented as mean ± SEM. * $p<0.05$, *** $p<0.005$, Veh. vs OCA groups by Holm-Sidak t-test.

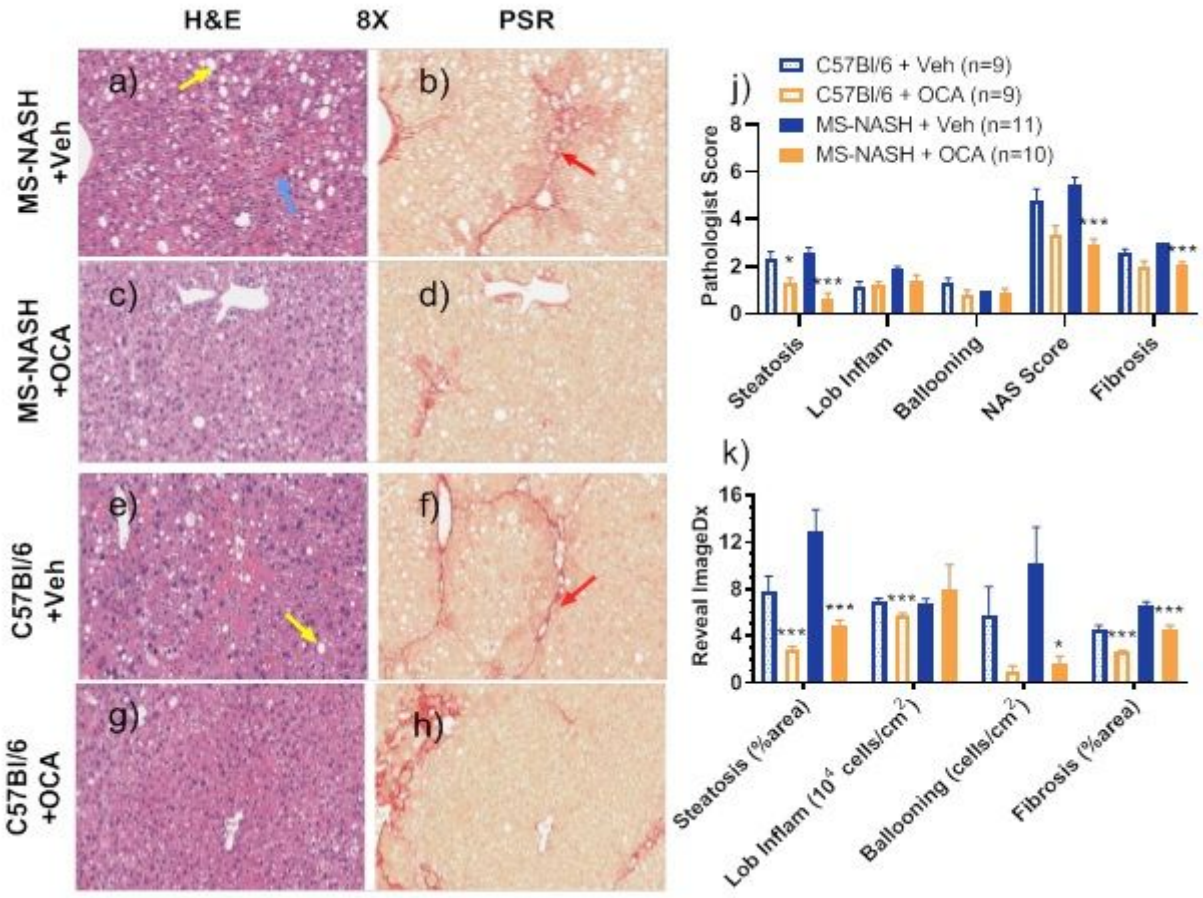


## Figure 6

Histopathology of Obeticholic acid (OCA, 30 mg/kg, QD) treatment on Western diet supplemented with fructose (WDF) fed MS-NASH or C57Bl/6 mice under low dose CCL4 (0.08 mL/kg) twice weekly for 8 weeks Left panel: Representative images of H&E and PSR staining in MS-NASH mice on WDF treated with (a & b) vehicle or (c & d) OCA or C57Bl/6 mice with (e & f) vehicle or (g & h) OCA. Yellow arrows indicate steatosis, blue arrows indicate microvesicular ballooning, and red arrows indicate fibrosis. Top right panel (j): Pathologist scores of steatosis (0-3), lobular inflammation (0-3), ballooning (0-2) and NAFLD Activity (0-8), as well as fibrosis (0-4). Bottom right panel (k): Quantitative imaging analysis of steatosis, inflammatory cell infiltration, hepatic ballooning and fibrosis by Reveal ImageDx software. Data represented as mean ± SEM. * $p<0.05$, *** $p<0.005$, Veh VS OCA group using Holm-Sidak t-test.

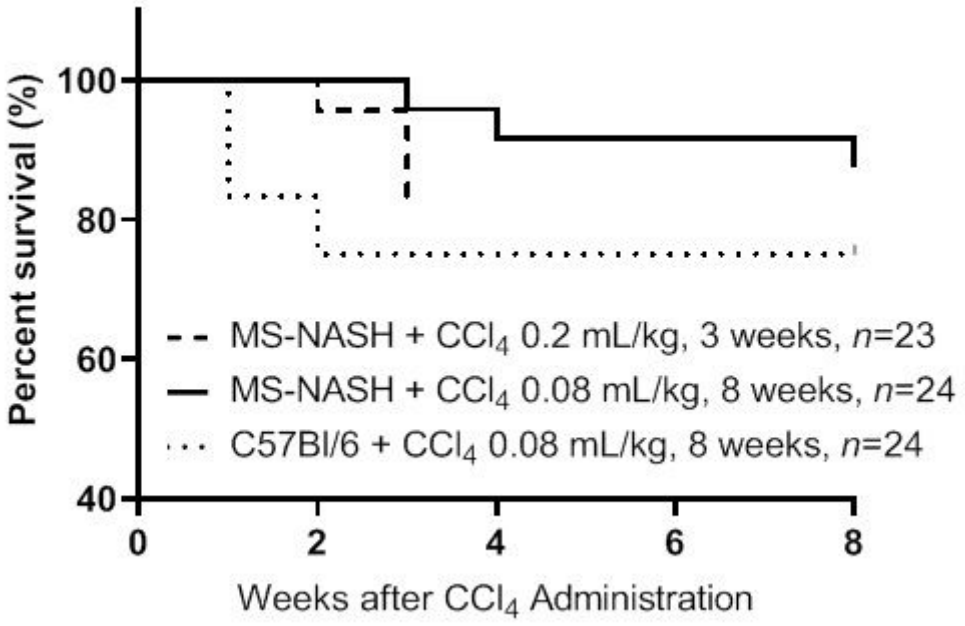


**Figure 7**

Comparison of survival rates in Western diet supplemented with fructose (WDF) fed MS-NASH or C57Bl/6 mice under CCl4 twice weekly.

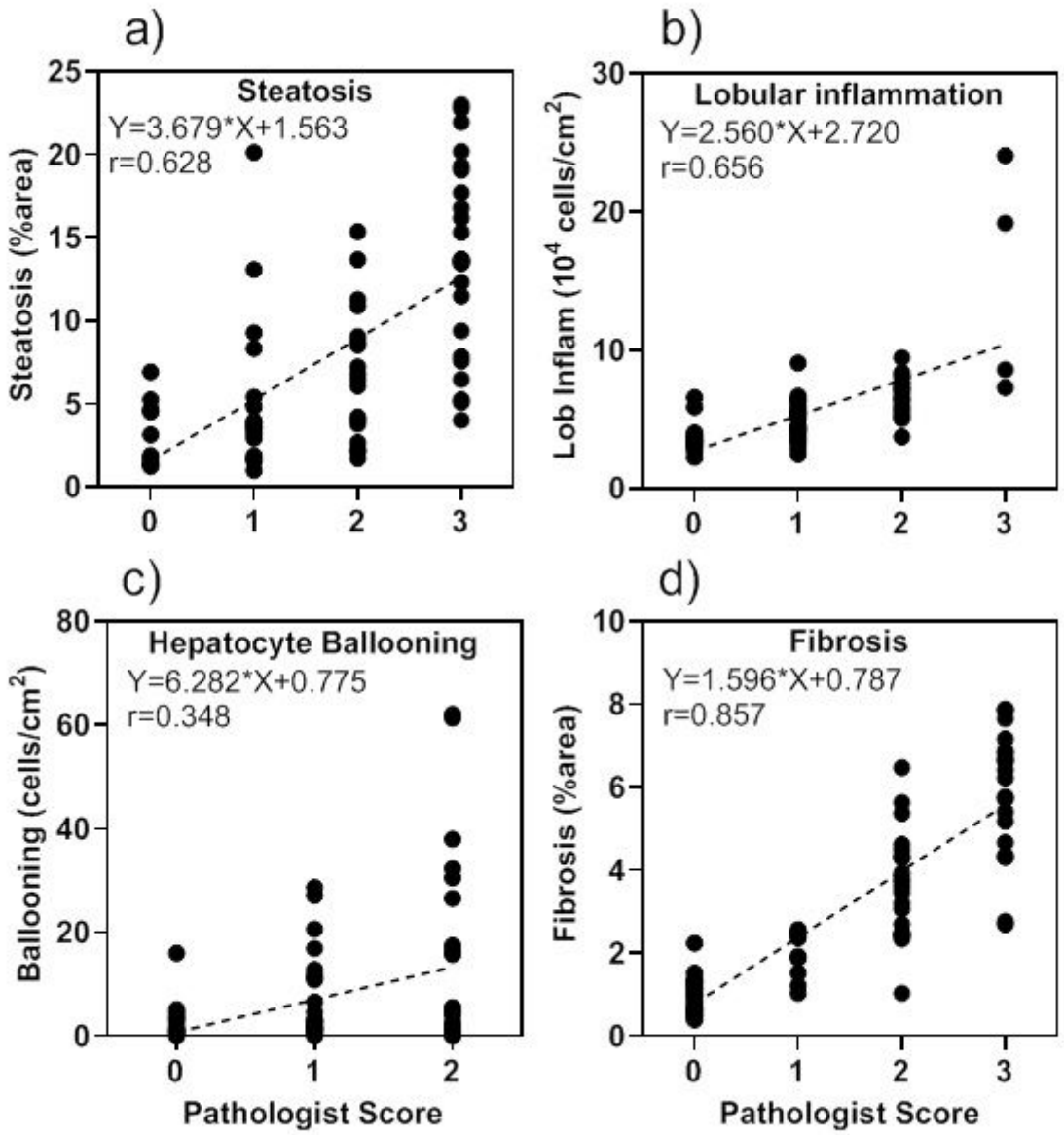


**Figure 8**

Correlation between Pathology scores and Reveal ImageDx analysis Correlations between pathology scores for (a) Steatosis; (b) lobular inflammation; (c) hepatocyte ballooning; and (d) fibrosis and Reveal ImageDx quantification by simple linear correlation with Pearson's coefficients. All the Pearson correlation coefficient r values are statistically significant.

# Supplementary Files

This is a list of supplementary files associated with this preprint. Click to download.

- 20200518MinimumStandardsofReportingChecklist.docx
- NC3RsARRIVEGuidelinesChecklist2014.docx